

# Ten Years of *Swift*: a Universal Scaling for Short and Long Gamma-Ray Bursts ( $E_{X,iso}$ - $E_{\gamma,iso}$ - $E_{pk}$ )

Elena Zaninoni<sup>1,a)</sup>, Maria Grazia Bernardini<sup>2</sup>, Raffaella Margutti<sup>3</sup> and Lorenzo Amati<sup>4</sup>

<sup>1</sup>*ICRANet-Rio, Centro Brasileiro de Pesquisas Físicas, Rua Dr. Xavier Sigaud 150, 22290-180 Rio de Janeiro, Brazil*

<sup>2</sup>*INAF - Osservatorio Astronomico di Brera, via Bianchi 46, Merate 23807, Italy*

<sup>3</sup>*Harvard-Smithsonian Center for Astrophysics, 60 Garden Street, Cambridge, MA02138*

<sup>4</sup>*INAF, Istituto di Astrofisica Spaziale e Fisica Cosmica, Bologna, Via Gobetti 101, I-40129 Bologna, Italy*

<sup>a)</sup>Corresponding author: elena.zaninoni@gmail.com

**Abstract.** From the comprehensive statistical analysis of *Swift* X-ray light-curves collected from the launch of the *Swift* satellite until the end of 2010, we found a three-parameter correlation between the isotropic energy emitted in the rest frame 1-10<sup>4</sup> keV energy band during the prompt emission ( $E_{\gamma,iso}$ ), the rest frame peak of the prompt emission energy spectrum ( $E_{pk}$ ), and the X-ray energy emitted in the rest frame 0.3-30 keV observed energy band ( $E_{X,iso}$ ), computed excluding the contribution of the flares. The importance of this scaling law is that it is followed by both long and short GRBs, and, at the same time, involves prompt and afterglow emission quantities. Therefore there are some properties which are shared by long and short GRBs as a whole. We updated this correlation considering all GRBs observed until June 2014, confirming the existence of this scaling law, and examining some particular GRBs, as 090426 and 100816A. We also discuss the physics that is driving this correlation.

## INTRODUCTION

The *Swift* satellite [1], launched on November 2004, opened a new era for the study and understanding of gamma-ray bursts (GRBs), detecting more than 900 objects until January 2015. Thanks to its unique observing capabilities, many correlations involving prompt and afterglow emission quantities could be further investigated (e.g. [2, 3, 4, 5, 6]).

From the comprehensive statistical analysis of *Swift* X-ray light-curves collected from December 2004 until December 2010 ([7], hereafter M13), we found a three-parameter correlation between the isotropic energy emitted in the rest frame 1-10<sup>4</sup> keV energy band during the prompt emission ( $E_{\gamma,iso}$ ), the rest frame peak of the prompt emission energy spectrum ( $E_{pk}$ ), and the X-ray energy emitted in the rest frame 0.3-30 keV observed energy band ( $E_{X,iso}$ ), computed excluding the contribution of the flares. The uniqueness of this correlation is that accommodates long, short, and low-energetic GRBs, and, at the same time, involves prompt and afterglow emission quantities, suggesting that there are some properties which are shared by the GRB class as a whole ([8], hereafter B12, M13).

We considered all GRBs observed until June 2014 and, as in M13, we selected only GRBs that have: i) secure redshift measurement; ii) measured  $E_{pk}$ ; iii) complete X-ray light-curve<sup>1</sup>. In this way, we obtained a new sample composed of 81 long GRBs, 11 short GRBs and 2 GRBs with uncertain classification<sup>2</sup>. The new sample contains ~35% more GRBs than the previous one; in particular the sample of short GRBs doubled (Table 1).

This new sample gives us the possibility to better investigate: i) the role of short GRBs in the  $E_{X,iso}$ - $E_{\gamma,iso}$ - $E_{pk}$  correlation; ii) the properties of the group of GRBs that lies between long and short GRBs (which we call *intermediate group*); iii) the characteristics of peculiar GRBs, like ultra-long GRBs.

Uncertainties are given at 68 per cent confidence level (c.l.) unless explicitly mentioned. Standard cosmological quantities have been adopted:  $H_0 = 70 \text{ km s}^{-1} \text{ Mpc}^{-1}$ ,  $\Omega_\Lambda = 0.7$  and  $\Omega_M = 0.3$ .

<sup>1</sup>Promptly re-pointed by *Swift*/XRT ( $t_{rep} \leq 300 \text{ s}$ ) and for which observations were not limited by any observing constraint (M13).

<sup>2</sup>GRBs with uncertain classification are GRB 090426 and GRB 100816A. A detailed discussion can be found afterwards.

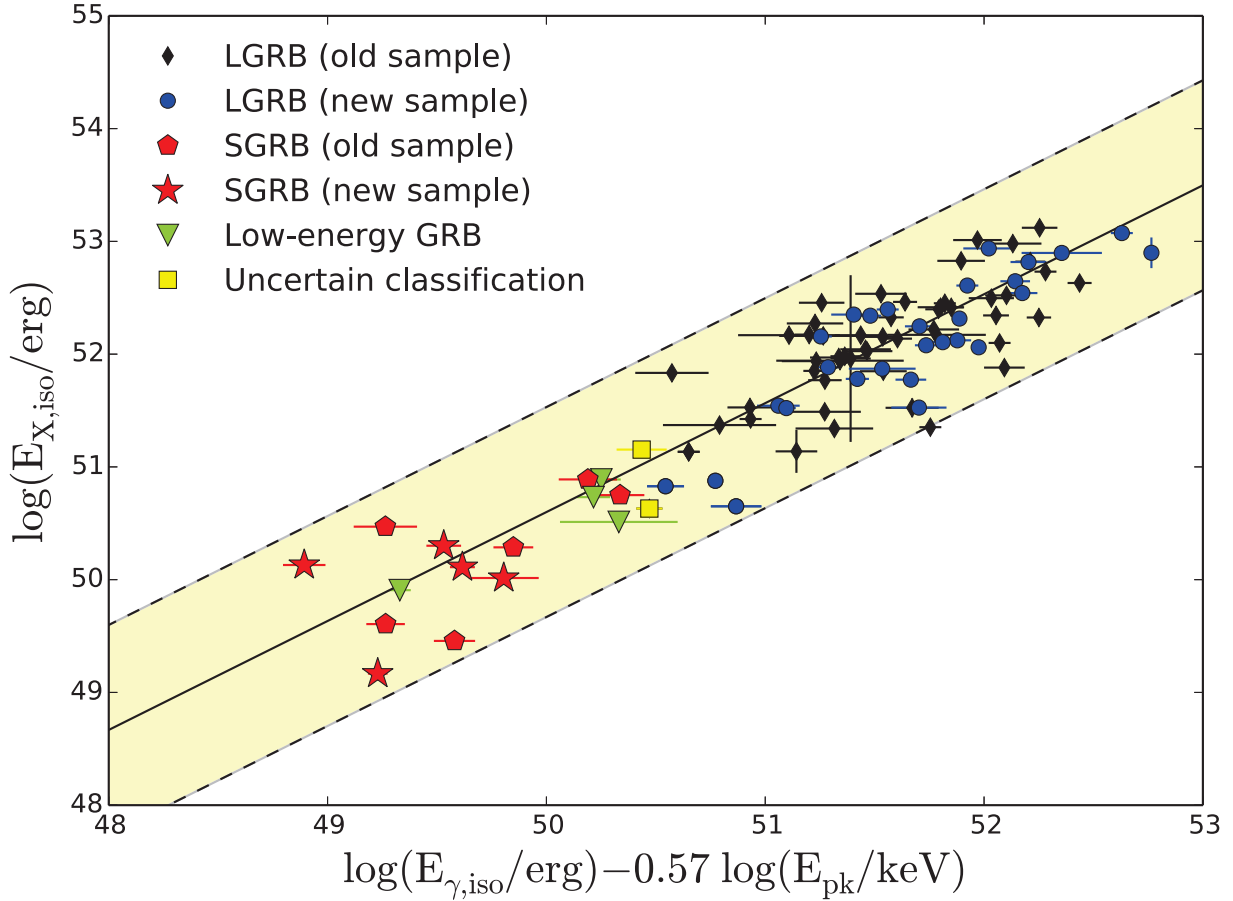


FIGURE 1:  $E_{X,iso} - E_{\gamma,iso} - E_{pk}$  correlation for the sample of 81 long GRBs (*black diamonds* for the old sample, *blue dots* for the new sample, and *green triangles* for low-energy GRBs), 11 short GRBs (*red pentagons* for the old sample and *red stars* for the new sample), and two GRBs with uncertain classification (*yellow squares*). The *black solid line* is the best-fitting function  $\text{Log}[E_{X,iso}] = 0.96 \text{Log}[E_{\gamma,iso}] - 0.57 \text{Log}[E_{pk}] - 0.62$  and the *yellow area* marks the  $2\sigma$  confidence region.

### THE THREE-PARAMETER CORRELATION

The three-parameter correlation involves  $E_{X,iso}$ ,  $E_{\gamma,iso}$ , and  $E_{pk}$ .  $E_{pk}$  and  $E_{\gamma,iso}$  are calculated as described in [3]. For short GRBs 080123, 090423, 100625A, 111117A, and 130603B, we consider the values of  $E_{pk}$  and  $E_{\gamma,iso}$  reported in [9].  $E_{X,iso}$  is the X-ray energy emitted in the 0.3-30 keV band in the rest frame and we calculated it as in M13.

The correlation is derived using the method of D'Agostini [10], which considers an intrinsic scatter  $\sigma_{ext}$  that accounts for the possible contribution of hidden variables. We obtained:

$$\text{Log} \left[ \frac{E_{X,iso}}{\text{erg}} \right] = (0.97 \pm 0.06) \text{Log} \left[ \frac{E_{\gamma,iso}}{\text{erg}} \right] - (0.57 \pm 0.13) \text{Log} \left[ \frac{E_{pk}}{\text{keV}} \right] - (0.62 \pm 0.08), \quad (1)$$

with an extra-scatter  $\sigma_{ext} = 0.32 \pm 0.04$ . Figure 1 shows a two-dimension representation of this relation respect to observations. As explained in previous papers (B12, M13), this correlation is robust, spanning four orders of magnitude in  $E_{X,iso}$  and  $E_{pk}$ , and six orders of magnitude in  $E_{\gamma,iso}$ , and combines both short and long GRBs in a common scaling.

TABLE 1: List of 33 GRBs added to the old sample. Short GRBs are marked in boldface, while GRB with uncertain classification is underlined.

GRB name
<b>080123</b> , <u>090426</u> , <b>100117A</b> , <b>100625A</b> , 110106B, 110205A, 110213A, 110503A, 110715A, 110731A, 110801A, 110818A, 111107A, <b>111117A</b> , 111209A, 111228A, 120119A, 120326A, 120712A, 120802A, 120811C, 121128A, 130408A, 130427A, 130505A, <b>130603B</b> , 130701A, 130831A, 130907A, 130925A, 131030A, 140206A, 140419A

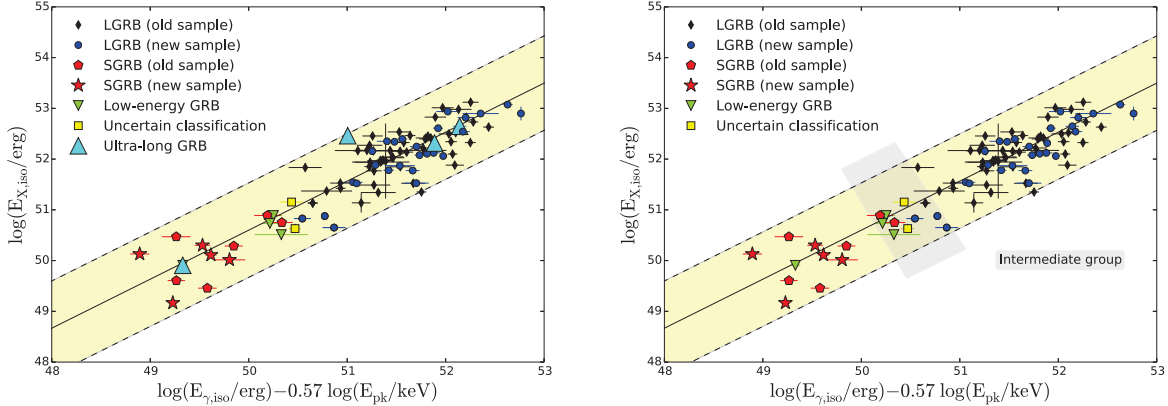


FIGURE 2:  $E_{X,iso} - E_{\gamma,iso} - E_{pk}$  correlation. Color code as Figure 1. *Left*: cyan triangles indicate the ultra-long GRBs we consider in our discussion: 060218, 101225A, 111209A, 130925A. *Right*: the gray area indicates the position of the intermediate group.

### Ultra-long GRBs

Recently, there has been extensive discussion about the existence of a new class of GRBs, named ultra-long GRBs (e.g. [11, 12, 13, 14, 15, 16]). We consider as ultra-long GRBs, those bursts with durations of several thousand seconds (e.g. [16, 13]). In our sample there are three ultra long lasting bursts: low-energy<sup>3</sup> GRB 060218 and GRBs 111209A and 130925A. In what follows we consider also GRB 101225A, which was not considered in our previous sample because of the uncertainty of its redshift [17, 11], now settled to be 0.847 [16].

Ultra-long GRBs (Figure 2, *left*, cyan triangles) are consistent with the  $E_{X,iso} - E_{\gamma,iso} - E_{pk}$  correlation as all other GRBs. Even if these GRBs seem to show uncommon local properties (e.g. [16]), their similar behavior in the  $E_{X,iso} - E_{\gamma,iso} - E_{pk}$  correlation could be related to a general and not local feature, as the dynamics of the jet.

### GRBs with uncertain classification

GRBs 090426 and 100816A have an uncertain classification, because they show properties that are intermediate between long and short GRBs. From Figure 1, we note that short GRBs occupy the left bottom part of the correlation plane, instead GRB 090426 lies between the groups of long and short GRBs. Indeed the classification of this GRB is very debated (e.g., [18, 19, 20, 21, 22, 9]). GRB 090624 has a very soft spectral index and it lies in the  $2\sigma$  confidence level region of the Amati relation, as long GRBs (Figure 3, *left*). On the other hand, its gamma-ray emission duration is less than 2 s ( $T_{90}^{obs} < 0.2$  s and  $T_{90}^{RF} < 0.5$  s)<sup>4</sup>. In addition, the value of the intrinsic absorption ( $N_H = 2.3_{-19}^{+5.6} \times 10^{21}$  cm<sup>-2</sup>), the presence of the highly ionized absorption lines, the position of the afterglow in the host galaxy, and the duration of the gamma-ray emission, support the idea that GRB 090426 was formed by the merger of two compact objects (e.g. [23, 24]).

GRB 100816A lies between long and short GRB groups in the  $E_{X,iso} - E_{\gamma,iso} - E_{pk}$  correlation and its classification is still uncertain [25, 26, 7, 9]. It can be classified as short GRB because it has a hard spectrum, it lies offset from its

<sup>3</sup>We consider as low-energy GRBs long GRBs with  $E_{\gamma,iso}$  below  $10^{52}$  erg.

<sup>4</sup> $T_{90}$  is the time in which from 5% to 95% cumulative counts are recorded.

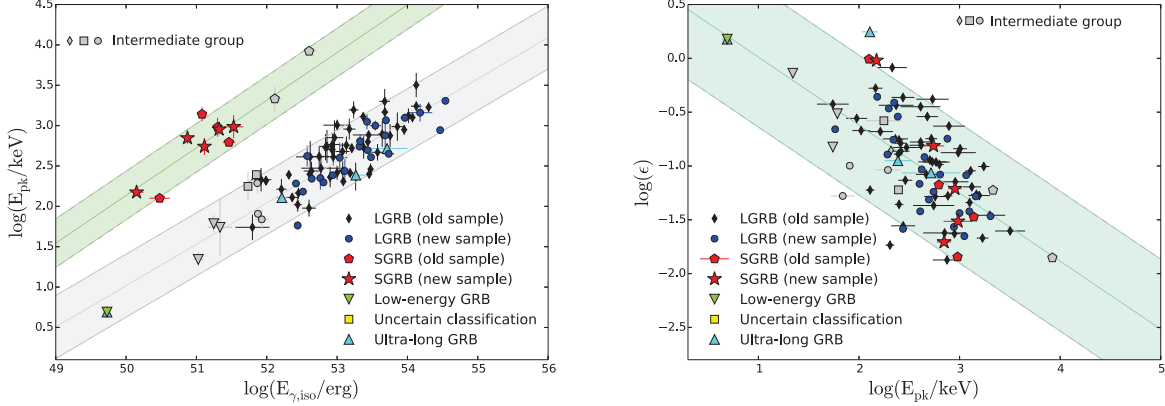


FIGURE 3: Color code as Figure 1. *Gray* symbols indicate the intermediate group. *Left*: the Amati relation ( $E_{\gamma,iso} - E_{pk}$  relation): the *green* solid line is the best fit function for short GRBs as calculated by Calderone *et al.* [28] and the *green* area marks the  $2\sigma$  region. The *gray* area indicates that the best fit is computed using only long GRBs. *Right*:  $E_{pk}$  vs.  $\epsilon$  relation. The *cyan* area indicates that the best fit is computed using all GRBs of the sample.

host galaxy, and there is no association with a supernova (SN). On the other hand, in strict analogy to long GRBs, it follows the Amati relation (Figure 3, *left*), its gamma-ray duration is longer than 2 s ( $T_{90} \sim 2.9$  s), and has a positive spectral lag [27].

### The intermediate group

In the previous compilation of the  $E_{X,iso} - E_{\gamma,iso} - E_{pk}$  correlation, GRBs were divided in two groups along the correlation with a lack of objects between them. Thanks to the updated sample, this area is now occupied by three new long GRBs (110106B, 120724A, 130831A) and a GRB with uncertain classification (090426). This group of objects, together with short GRBs 070714B and 090510, low-energy GRBs 050416A, 060614, and 081007, long GRB 080916, and GRB 100816A with uncertain classification, suggest the presence of an intermediate group between long and short GRBs (Figure 2, *right*, *gray area*).

In the Amati relation (Figure 3, *left*) the intermediate group lies in the low peak energy part of the plane, with the exception of two short GRBs, since the Amati relation is followed only by long GRBs. GRB 090426 and GRB 100816A are within in the limit of  $2\sigma$  of the Amati relation, so they behave as long GRBs [9].

The GRBs of the intermediate group have small redshifts, like short GRBs, and are less energetic than long one, even if they have typical long GRB durations. They have canonical X-ray light-curves and they show limited flaring activity. Therefore they seem to represent a transitional group between GRBs with low energies and simple X-ray light-curves (e.g. single or double power laws or canonical shapes) and more energetic long GRBs, with also complex and unusual X-ray light-curves (e.g. with a shallow phase before the steep decay or with big flares). A larger sample is needed to confirm or rule out the presence of an intermediate group.

### Possible biases

In B12 and M13 we discussed the possible caveat on the definition of  $E_{X,iso}$ . In particular, we analysed the differences between the values computed in the observer frame 0.3-10 keV and in the rest frame 0.3-30 keV, on the arbitrariness of the choice of the interval time for the integration, and the inclusion of flares in the computation of the  $E_{X,iso}$ . We concluded that these factors do not influence the  $E_{X,iso} - E_{\gamma,iso} - E_{pk}$  correlation.

In Figure 4 (*left*), we show the distribution of GRBs in the  $E_{\gamma,iso} - E_{pk} - E_{X,iso}$  plane depending on their redshift  $z$ . Low X-ray energy GRBs (short GRBs and low-energy long GRBs) are observed only at low redshift, while long GRBs are observed at every redshift. As expected, there is not a redshift trend in the distribution of GRBs in this plane, therefore we can exclude that this parameter could influence the  $E_{X,iso} - E_{\gamma,iso} - E_{pk}$  correlation.

We consider the possibility that the  $E_{X,iso} - E_{\gamma,iso} - E_{pk}$  correlation could be influenced by the different morphology

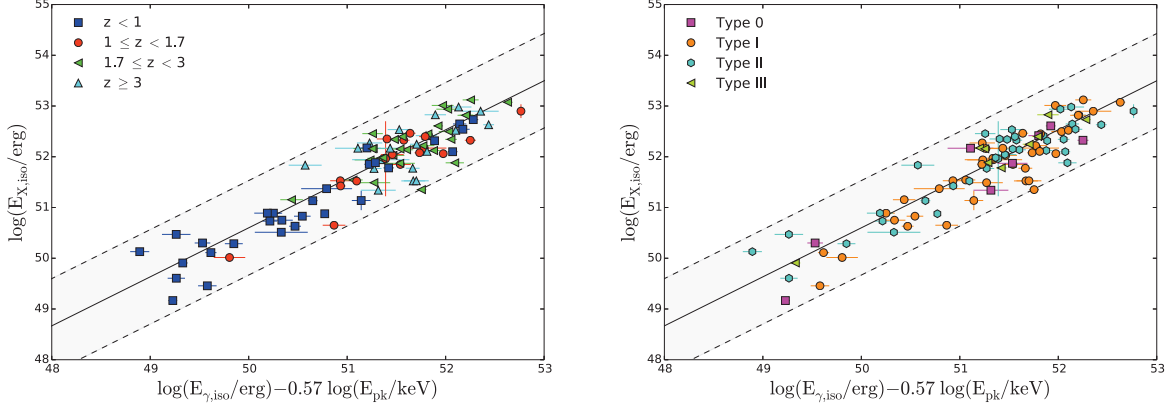


FIGURE 4:  $E_{X,\text{iso}}-E_{\gamma,\text{iso}}-E_{\text{pk}}$  correlation, considering the differences in redshift (*left*) and in X-ray light-curve morphology (*right*) for GRBs in our sample. The *black solid line* is the best fit function, as in Figure 1, and the *gray area* marks the  $2\sigma$  regions.

of the X-ray light-curve<sup>5</sup>. Since GRBs with different X-ray light-curve shape are equally distributed on the plane (Figure 4, *right*), we conclude that the distribution of GRBs in the  $E_{X,\text{iso}}-E_{\gamma,\text{iso}}-E_{\text{pk}}$  plane is not dependent on this feature.

## Physics and models

For a GRB event, the efficiency of the process is defined as the ratio between the prompt emission energy and the outflow kinetic energy (e.g., [29]). Since the kinetic energy could be computed considering the afterglow emission, we define the inverse of the efficiency as  $\epsilon = E_{\gamma,\text{iso}} / E_{X,\text{iso}}$  and we plot this quantity against the peak energy  $E_{\text{pk}}$  (Figure 3, *right*). As we showed in our previous works (B12, M13), we have two new groups: one of low-energetic GRBs which are less efficient and occupy the top left part of the plane, and the other group composed of short and long GRBs, which have similar efficiencies. From this plot we can see that GRBs of the intermediate group share the area with efficient bursts. The physical origin of such a relation may be connected with the outflow Lorentz factor (B12, M13).

The physics behind the prompt emission is still one of the main open issues in the study of GRBs, with several emission mechanisms and scenario being proposed. Among these, the photospheric models (e.g. [30]) and the cannonball (CB) model (e.g. [31]) are the ones providing most naturally a physical ground to the  $E_{X,\text{iso}}-E_{\gamma,\text{iso}}-E_{\text{pk}}$  correlation.

The photospheric model considers how the GRB spectrum in the optically thick phase can be modified by the interaction of the radiation field with the leptonic component of the outflow, before it is released at the photosphere [30, 32, 33, 34]. The simulations made by Lazzati et al. [35] can reproduce the three-parameter correlation since the radiative efficiency of brighter bursts is higher than that of weaker bursts. However, for adequately comparing the observations and the simulations, it is necessary to assume a fiducial value for the electron equipartition parameter  $\epsilon = 0.1$  [35].

In the cannonball model [31, 36, 37], the Inverse Compton scattering caused by the interaction between electrons of the CB plasma and the light in the near ambient of the SN is responsible of the gamma-ray prompt emission of GRBs, while the afterglow emission is related to the synchrotron radiation of electrons swept-in and accelerated in the CBs. In this model, the three-parameter correlation is simply the combination of the two parameter correlations of kinetic origin that are followed by both long and short GRBs, even if with different normalizations, and so it depends on the large Doppler boosting and the relativistic beaming that strongly influenced the observed radiation [38].

<sup>5</sup>We classify the X-ray light-curves basing on the number of break times in their fitting function (M13): *Type 0* is fitted with a single power-law, *Type 1* with the sum of two power-laws, *Type II* (or *canonical*) with the sum of three power-laws, and *Type III* with the sum of four power-laws.

## SUMMARY AND CONCLUSIONS

In this work we updated the three-parameter correlation (B12, M13) considering GRBs detected until June 2014: the new sample contains about 35% more GRBs than the original one, and, in particular, the number of short GRBs doubles (81 long GRBs, 11 short GRBs, and 2 GRBs with uncertain classification). The main results are:

- This correlation involves both prompt and afterglow quantities ( $E_{X,iso}$ ,  $E_{\gamma,iso}$  and  $E_{pk}$ ) and it is followed by all kinds of GRBs, both short and long GRBs.
- It implies the existence of common properties between long, short and low energetic GRBs, even if they have different progenitors and environments.
- This correlation is followed also by ultra-long GRBs (060218, 101225A, 111209A, and 130925A).
- There is a possible intermediate group of transition between long and short GRBs, composed by different kinds of GRBs.
- It is not influenced by: the definition of  $E_{X,iso}$ , the redshift  $z$  and the X-ray light curve morphology.
- This correlation can be expressed in the form of a two-parameter correlation between the GRB efficiency and  $E_{pk}$ . The physical origin of such a relation may be connected with the outflow Lorentz factor.
- The photospheric model and the CB model can reproduce this correlation.

A detailed description and analysis of the three-parameter correlation and its implications will be presented in Zaninoni et al. (submitted to MNRAS).

## ACKNOWLEDGMENTS

This work made use of data supplied by the UK Swift Science Data Centre at the University of Leicester. EZ thanks Luca Izzo and Marco Muccino for sharing their data. EZ acknowledges the support by the International Cooperation Program CAPES-ICRANet financed by CAPES - Brazilian Federal Agency for Support and Evaluation of Graduate Education within the Ministry of Education of Brazil. MGB thanks support from T-Rex Program.

## REFERENCES

- [1] N. Gehrels, G. Chincarini, P. Giommi, K. O. Mason, J. A. Nousek, A. A. Wells, N. E. White, S. D. Barthelmy, D. N. Burrows, L. R. Cominsky, and a. et, *ApJ* **611**, 1005–1020 (2004).
- [2] D. E. Reichart, D. Q. Lamb, E. E. Fenimore, E. Ramirez-Ruiz, T. L. Cline, and K. Hurley, *ApJ* **552**, 57–71 (2001).
- [3] L. Amati, F. Frontera, M. Tavani, J. J. M. in't Zand, A. Antonelli, E. Costa, M. Feroci, C. Guidorzi, J. Heise, N. Masetti, E. Montanari, L. Nicastro, E. Palazzi, E. Pian, L. Piro, and P. Soffitta, *A&A* **390**, 81–89 (2002).
- [4] G. Ghirlanda, G. Ghisellini, and D. Lazzati, *ApJ* **616**, 331–338 (2004).
- [5] D. Yonetoku, T. Murakami, T. Nakamura, R. Yamazaki, A. K. Inoue, and K. Ioka, *ApJ* **609**, 935–951 (2004).
- [6] M. G. Dainotti, V. F. Cardone, and S. Capozziello, *MNRAS* **391**, L79–L83 (2008).
- [7] R. Margutti, E. Zaninoni, M. G. Bernardini, G. Chincarini, and a. et, *MNRAS* **428**, 729–742 (2013).
- [8] M. G. Bernardini, R. Margutti, E. Zaninoni, and G. Chincarini, *MNRAS* **425**, 1199–1204 (2012).
- [9] P. D'Avanzo, R. Salvaterra, M. G. Bernardini, L. Nava, S. Campana, S. Covino, V. D'Elia, G. Ghirlanda, G. Ghisellini, A. Melandri, B. Sbarufatti, S. D. Vergani, and G. Tagliaferri, *MNRAS* **442**, 2342–2356 (2014).
- [10] G. D'Agostini, ArXiv Physics e-prints (2005), [physics/0511182](https://arxiv.org/abs/physics/0511182).
- [11] C. C. Thöne, A. de Ugarte Postigo, C. L. Fryer, K. L. Page, J. Gorosabel, M. A. Aloy, D. A. Perley, C. Kouveliotou, H. T. Janka, P. Mimica, J. L. Racusin, H. Krimm, J. Cummings, S. R. Oates, S. T. Holland, and M. H. Siegel, *Nature* **480**, 72–74 (2011).
- [12] B. Gendre, J. L. Atteia, M. Boër, F. Colas, A. Klotz, F. Kugel, M. Laas-Bourez, C. Rinner, J. Strajnic, G. Stratta, and F. Vachier, *ApJ* **748**, p. 59 (2012).
- [13] B. Gendre, G. Stratta, J. L. Atteia, S. Basa, M. Boër, D. M. Coward, S. Cutini, V. D'Elia, E. J. Howell, A. Klotz, and L. Piro, *ApJ* **766**, p. 30 (2013).
- [14] F. J. Virgili, C. G. Mundell, V. Pal'shin, C. Guidorzi, R. Margutti, A. Melandri, R. Harrison, S. Kobayashi, and R. Chornock, *ApJ* **778**, p. 54 (2013).
- [15] B.-B. Zhang, B. Zhang, K. Murase, V. Connaughton, and M. S. Briggs, *ApJ* **787**, p. 66 (2014).

- [16] A. J. Levan, N. R. Tanvir, R. L. C. Starling, K. Wiersema, K. L. Page, D. A. Perley, S. Schulze, G. A. Wynn, R. Chornock, J. Hjorth, S. B. Cenko, A. S. Fruchter, P. T. O’Brien, G. C. Brown, R. L. Tunnicliffe, D. Malesani, P. Jakobsson, D. Watson, E. Berger, D. Bersier, B. E. Cobb, S. Covino, A. Cucchiara, A. de Ugarte Postigo, D. B. Fox, A. Gal-Yam, P. Goldoni, J. Gorosabel, L. Kaper, T. Krühler, R. Karjalainen, J. P. Osborne, E. Pian, R. Sánchez-Ramírez, B. Schmidt, I. Skillen, G. Tagliaferri, C. Thöne, O. Vaduvescu, R. A. M. J. Wijers, and B. A. Zauderer, *ApJ* **781**, p. 13 (2014).
- [17] S. Campana, G. Lodato, P. D’Avanzo, N. Panagia, E. M. Rossi, M. Della Valle, G. Tagliaferri, L. A. Antonelli, S. Covino, G. Ghirlanda, G. Ghisellini, A. Melandri, E. Pian, R. Salvaterra, G. Cusumano, V. D’Elia, D. Fugazza, E. Palazzi, B. Sbarufatti, and D. S. Vergani, *Nature* **480**, 69–71 (2011).
- [18] L. A. Antonelli, P. D’Avanzo, R. Perna, L. Amati, S. Covino, S. Cutini, V. D’Elia, S. Gallozzi, A. Grazian, and E. Palazzi, *A&A* **507**, L45–L48 (2009).
- [19] E. Levesque, J. S. Bloom, N. R. Butler, D. A. Perley, S. B. Cenko, J. X. Prochaska, L. J. Kewley, A. Bunker, H.-W. Chen, R. Chornock, A. V. Filippenko, K. Glazebrook, S. Lopez, J. Masiero, M. Modjaz, A. Morgan, and D. Poznanski, *MNRAS* **401**, 963–972 (2010).
- [20] C. C. Thöne, S. Campana, D. Lazzati, A. de Ugarte Postigo, J. P. U. Fynbo, L. Christensen, A. J. Levan, M. A. Aloy, and J. Hjorth, *MNRAS* **414**, 479–488 (2011).
- [21] A. Nicuesa Guelbenzu, S. Klose, A. Rossi, D. A. Kann, T. Krühler, J. Greiner, A. Rau, F. Olivares E., P. M. J. Afonso, R. Filgas, and A. Küpcü Yoldaş, *A&A* **531**, p. L6 (2011).
- [22] D. Grupe, J. A. Nousek, P. Veres, B.-B. Zhang, and N. Gehrels, *ApJS* **209**, p. 20 (2013).
- [23] K. Belczynski, R. Perna, T. Bulik, V. Kalogera, N. Ivanova, and D. Q. Lamb, *ApJ* **648**, 1110–1116 (2006).
- [24] R. Perna and K. Belczynski, *ApJ* **570**, 252–263 (2002).
- [25] R. L. Tunnicliffe and A. Levan, “GRB 100816A and the nature of intermediate duration gamma-ray bursts,” in *Death of Massive Stars: Supernovae and Gamma-Ray Bursts*, IAU Symposium, Vol. 279 (2012), pp. 415–416.
- [26] J. P. Norris, N. Gehrels, and J. D. Scargle, *ApJ* **735**, p. 23 (2011).
- [27] M. G. Bernardini, G. Ghirlanda, S. Campana, S. Covino, R. Salvaterra, J.-L. Atteia, D. Burlon, G. Calderone, P. D’Avanzo, V. D’Elia, G. Ghisellini, V. Heussaff, D. Lazzati, A. Melandri, L. Nava, S. D. Vergani, and G. Tagliaferri, *MNRAS* **446**, 1129–1138 (2015).
- [28] G. Calderone, G. Ghirlanda, G. Ghisellini, M. G. Bernardini, S. Campana, S. Covino, D. D’Avanzo, V., A. Melandri, R. Salvaterra, B. Sbarufatti, and G. Tagliaferri, *MNRAS* **448**, 403–416 (2015).
- [29] N. M. Lloyd-Ronning and B. Zhang, *ApJ* **613**, 477–483 (2004).
- [30] P. Mészáros and M. J. Rees, *ApJ* **530**, 292–298 (2000).
- [31] A. Dar and A. de Rújula, *Physics Reports* **405**, 203–278 (2004).
- [32] M. J. Rees and P. Mészáros, *ApJ* **628**, 847–852 (2005).
- [33] D. Giannios, *A&A* **457**, 763–770 (2006).
- [34] D. Lazzati, B. J. Morsony, and M. C. Begelman, *ApJ* **700**, L47–L50 (2009).
- [35] D. Lazzati, B. J. Morsony, R. Margutti, and M. C. Begelman, *ApJ* **765**, p. 103 (2013).
- [36] S. Dado, A. Dar, and A. De Rújula, *ApJ* **693**, 311–328 (2009).
- [37] S. Dado, A. Dar, and A. De Rújula, *ApJ* **696**, 994–1020 (2009).
- [38] S. Dado and A. Dar, *ApJ* **775**, p. 16 (2013).